The Impact of the Tropical Indian Ocean
on South Asian High in Boreal Summer

HUANG Gang[*1] (黄 刚), QU Xia[2,3] (屈 侠), and HU Kaiming[2,3] (胡开明)

[1]*Key Laboratory of Regional Climate-Environment Research for Temperate East Asia,*

Institute of Atmospheric Physics, Chinese Academy of Sciences, Beijing 100029

[2]*State Key Laboratory of Numerical Modeling for Atmospheric Sciences and Geophysical*

Fluid Dynamics, Center for Monsoon System Research, Institute of Atmospheric Physics,

Chinese Academy of Sciences, Beijing 100083

[3]*Graduate University of Chinese Academy of Sciences, Beijing* 100049

ABSTRACT

The tropical Indian Ocean (TIO) is warmer than normal during the summer when or after the El Niño decays. The present study investigates the impact of TIO SST on the South Asian High (SAH) in summer. When the TIO is warmer, the SAH strengthens and its center shifts southward. It is found that the variations in the SAH cannot be accounted for by the precipitation anomaly. A possible mechanism is proposed to explain the connection between the TIO and SAH: warmer SST in the TIO changes the equivalent potential temperature (EPT) in the atmospheric boundary layer (ABL), alters the temperature profile of the moist atmosphere, warms the troposphere, which produces significant positive height anomaly over South Asia and modifies the SAH.

An atmospheric general circulation model, ECHAM5, which has a reasonable prediction skill in the TIO and South Asia, was selected to test the effects of TIO SST on the SAH. The experiment with idealized heating over the TIO reproduced the response of the SAH to TIO warming. The results suggest that the TIO-induced EPT change in the ABL can account for the variations in the SAH.

Key words: tropical Indian Ocean, South Asia High, equivalent potential temperature

1. Introduction

The ENSO is a major mode of air–sea interaction on interannual timescale with profound influences on global climate. The tropical Indian Ocean (TIO) gradually warms when El Niño is in its developing phase, and the warming reaches a maximum nearly one season after the NINO3.4 SST anomaly has peaked (Klein et al., 1999; Lau and Nath, 2000; Alexander et al., 2002; Lau and Nath, 2003). The warm anomaly still exists during the summer after the peak of El Niño (Du et al., 2009). Klein et al. (1999) pointed out that changes in evaporation and cloud cover induced by the El Niño account for the warm anomaly over most parts of the Indian Ocean during the ENSO decaying phase; while the warm anomaly over the southwest Indian Ocean could not be explained by the above changes. Previous research (Masumoto and Meyers, 1998; Yu et al., 2005) revealed that, when the ENSO matures, changes in the Walker circulation generate an anticyclonic wind anomaly over the TIO, which forces downwelling Rossby waves in the southeast Indian Ocean. The Rossby waves propagate westward, arrive in the southwest Indian Ocean several months later, deepen the thermocline ridge and warm the SST (Huang and Kinter, 2002; Xie et al., 2002). Thus, ocean dynam-

ics may play an important role in the warming in the southwest Indian Ocean.

The warming of the TIO in response to El Niño has influences on the climate locally and remotely after El Niño decays. This phenomenon is called the "capacitor effect" (Annamalai et al., 2005; Yang et al., 2007; Yang and Liu, 2008; Xie et al., 2009). In the years when there is basin-wide warming in the TIO, anticyclonic wind anomaly occurs over the western North Pacific, rainfall over Yangtze River is above normal and the South Asian High (SAH) strengthens in the summer (Yang et al., 2007). The Fast Ocean-Atmosphere Model and five Atmospheric General Circulation Models (AGCMs) have reproduced the phenomena (Yang et al., 2007; Li et al., 2008). Analysis by Xie et al. (2009) showed that a Kelvin wave anomaly induced by warming in TIO is key to the generation of an anticyclone anomaly over the western North Pacific. Earlier studies (Wang et al., 2000, 2003) suggested a role played by local air-sea interaction in the maintenance of the western North Pacific anomalous anticyclone in early summer.

Figures 1 and 2 demonstrate the regression of SST and 200-hPa velocity potential, respectively, on the NINO3.4 SST index from November(0) to January (N(0)D(0)J). The numeral "0" denote the preceding year. In the winter when El Niño peaks and the following spring, SST is warmer than normal in the equatorial eastern Pacific (EEP) and the 200-hPa velocity potential shows an upper-level anomalous divergence. Though there is a warming in the TIO, the 200-hPa velocity potential suggests a weak anomalous divergence or convergence over the TIO. This indicates that during these two seasons, the EEP SST has a major impact on circulation over the tropical Indo-Pacific Ocean and that TIO SST does not have a large impact on circulation or it just responds to the atmosphere passively. During the summer following El Niño, the warm anomaly over the EEP is weaker than that in N(0)D(0)J and March to May (MAM), and the intensity of the warm anomaly over the TIO is approximately equal to that in N(0)D(0)J and MAM. The 200-hPa velocity potential in summer shows an anomalous divergence over the TIO and no significant anomaly over the EEP, indicating an active role of the TIO SST on local and surrounding circulation in sum-
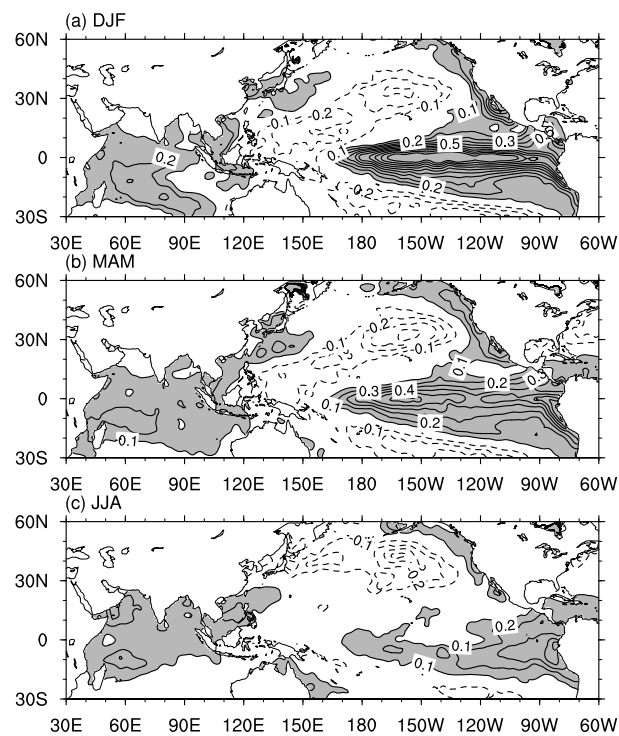

Fig. 1. Regression of SST against N(0)D(0)J NINO3.4 SST index from 1979–2007, (a), (b) and (c) are the results of D(0)JF, MAM and JJA, respectively. Negative values are shown in dash contours. Shading indicates values larger than 0.1; and the interval of white contours is 0.1 K, the unit is K. For the sake of clarity, spatial 9-point smoothing is performed and the zero contour is omitted.
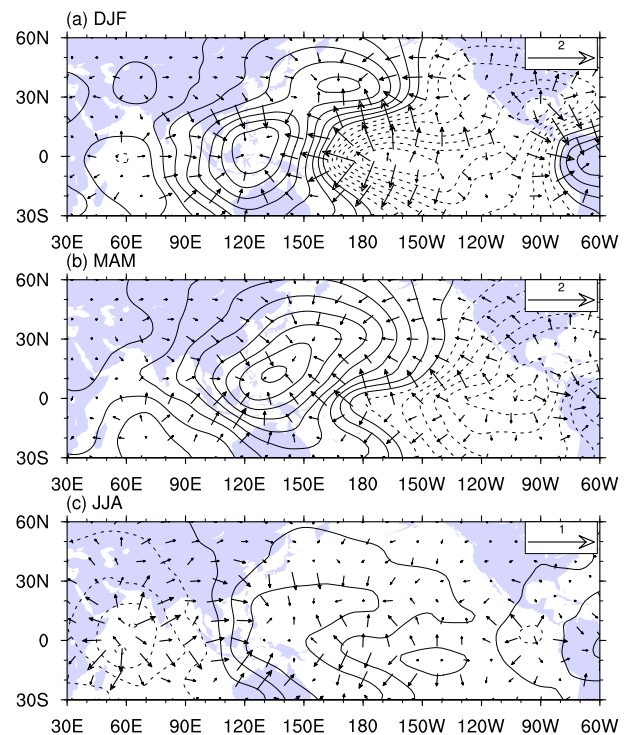

Fig. 2. As in Fig. 1, except for the results of 200-hPa velocity potential (contours) and divergent wind component (vectors), the contour interval is 2.5×10^5 m^2 s^{-1}. Solid and dashed lines represent positive and negative values, respectively.

mer, in agreement with Wu et al. (2009). The regression of SST and 200-hPa velocity potential in the preceding winter, spring, and summer, on the TIO SST in summer shows similar results. The present study focuses on the impacts of the TIO SST in summer.

The SAH is a high pressure system located in the upper troposphere over the Tibetan Plateau and its surrounding area in summer. It is a result of the elevated heating of the Tibetan Plateau to the atmosphere (Flohn, 1960) and has been recognized to be the strongest and steadiest system in the upper troposphere (Mason and Anderson, 1963). The variations of the SAH are tightly linked to precipitation and circulation over Asia. Tao and Zhu (1964) reported that longitudinal displacement of the SAH leads that of a 500-hPa subtropical anticyclone over the Western Pacific for a few days and is a good index for short- to medium-range weather forecasts in Asia. In the summer, when the SAH shifts eastward, significant positive rainfall anomalies occur in southern Japan, over the Korea Peninsula, and in the Yangtze River-Yellow River Valley of China and the Tibetan Plateau. As the SAH shifts westward, the rainfall over these areas tends to be below average (Zhang et al., 2002). Zhang and Wu (2001) pointed out there is a good relationship between the strength of the SAH and rainfall over the Yangtze River valley in summer. The variation of the summer SAH can modulate climate downstream. A strengthened SAH emanates anomalous wave energy downstream along the westerly jet stream, leading to the occurrence of an intensified subtropical high over the extratropical North Pacific (Zhao et al., 2009). Also, the summer SAH is linked to global circulation and precipitation. A strengthened SAH is accompanied by a strengthened and westward Western Pacific subtropical high, weakened mid-Pacific trough and strengthened Mexican high. Furthermore, rainfall tends to increase over South Asia, Central America, Australia and Central Africa, and decrease over the Pacific and Mediterranean (Zhang et al., 2005). In addition, the easterly and westerly jets residing on the south and north sides of the SAH form a transport barrier of some chemicals, such as water vapor and ozone (Dethof et al., 1999; Randel and Park, 2006). Meanwhile, because of upward transportation in the center of SAH, some chemicals such as carbon monoxide are transported to the upper troposphere and trapped there (Park et al., 2004; Li et al., 2005).

Because of the large heat content of water, warm oceans heat the atmosphere and exert deep influence on circulation. The TIO and SAH are adjacent in geographical position, and change in thermal regime over the TIO may affect the variability of the SAH. The Indian Ocean basin-wide mode strengthens the summer SAH probably through the Matsunuo-Gill response forced by condensational heating associated with increased precipitation over the TIO (Yang et al., 2007; Yang and Liu, 2008; Li et al., 2008).

In addition to changes in its strength, the SAH also varies in its latitudinal and longitudinal locations (Zhang et al., 2000, 2002). Although there have been studies on the relationship between the TIO SST and SAH strength, the impact of the TIO SST on the displacements of the SAH is not clear. At the same time, former studies on the effects of the TIO SST on the SAH do not clearly address the influencing mechanism. Our present analysis will show that precipitation over the TIO is not significantly correlated with TIO SST. The influence mechanism is therefore still not well understood, an issue that will be discuss further, below.

The paper is organized as follows. Section 2 describes data, the method and AGCM experiments. Section 3 analyses the effects of TIO SST on SAH variations and the possible influencing mechanism. Section 4 uses simulations to validate the relationship and influencing mechanism proposed in section 3. Section 5 presents a discussion and summary of the findings.

2. Data and method

2.1 *Observational data*

This study used the Hadley Center Global Sea Surface Temperature (HadISST) dataset (Rayner et al., 2006), the Center for Climate Prediction (CPC) Merged Analysis of Precipitation (CMAP; Xie and Arkin, 1997), and the National Centers for Environmental Prediction–National Center for Atmosphere Research (NCEP–NCAR) atmospheric reanalysis dataset (Kalnay et al., 1996). The horizontal grid resolutions of these datasets are $1° \times 1°$, $2.5° \times 2.5°$, and $2.5° \times 2.5°$, respectively. In order to be consistent with the period covered by the CMAP dataset which starts from 1979, and considering that there is interdecadal change in the influence of TIO SST during the late 1970s (Xie et al., 2010), the analysis and discussion in this paper will focus on the period 1979–2007.

Another focuses of the study is on the interannual variability of the TIO and SAH. For this purpose, three-month mean data were obtained and used in order to remove intraseasonal variability. Further, decadal and longer variations, which are significant over the TIO and surrounding areas (Du and Xie, 2008), were removed.

Correlation, regression and composite analysis were used to examine the relationship between the two variables. The statistical significance of a composite difference was assessed using the Student's t test. All
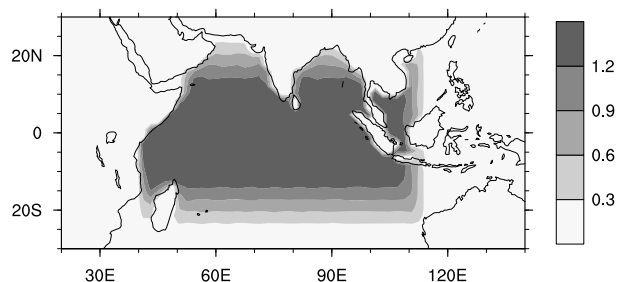
Fig. 3. Idealized SSTA imposed on climatological SST in ECHAM5.

Fig. 4. (a) Normalized TIO (20°S–20°N, 40°–100°E) SST in June–August from 1979–2007. (b) Contour lines for 100-hPa 16720 gpm geopotential height when TIO SST is warm (dashed line), cold (dotted line) and climatological (solid line) in JJA.

significances referred to in this paper are at the 95% confidence level, unless otherwise stated. Finally, summer, in the context of this study, refers to the period from June to August.

2.2 *AGCM experiment*

The AGCM was ECHAM5, the latest Hamburg version of the European Center for Medium-Range Weather Forecast model, with a resolution of T63L19 (Roeckner et al., 2003).

Two experiments were designed. The first used prescribed SST and sea-ice from 1957–1999 to drive ECHAM5 (hereafter, AMIP2). The results of this experiment will be used to examine the ability of the AGCM with respect to SAH and climate over the TIO and the surrounding regions. In order to be consistent with the period of observational analysis, a dataset with covering the period 1979–1999 was selected. In the second experiment, referred to as the TIO sensitivity experiment (TIOSE), the AGCM was driven by an idealized SST anomaly in the TIO superposed on the model's climatological monthly SST. The SST anomaly is maximum along the equator and gradually decreases to 0 at 30°N and 30°S (Fig. 3). The SST anomaly increases linearly at a rate of 0.2 K yr^{-1} from 0 to 2.2 K. Five simulations were performed with different initial conditions. In the discussion, the ensemble mean is analyzed to remove the uncertainties induced by the initial conditions and internal variability.

3. observations

3.1 *Relationship between TIO SST and the SAH*

Figure 4a illustrates normalized June–August (JJA) TIO (40°–100°N, 20°S–20°E) SST time series. Seven warm cases (1983, 1987, 1988, 1991, 1998, 2003, and 2007) and nine cold cases (1981, 1984, 1985, 1989, 1994, 1996, 1999, 2000, and 2004) were chosen when the JJA TIO SST index exceeded 0.5 and −0.5 stan-
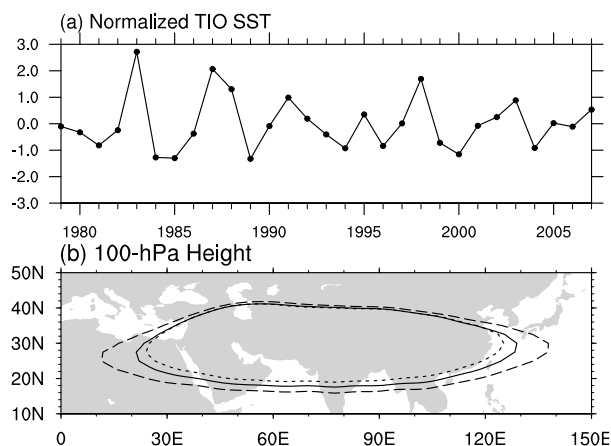
dard deviation, respectively.

Figure 4b shows contour lines for 16720 gpm of 100-hPa geopotential height when TIO SST represents warm cases (dashed contour line), cold cases (dotted contour line) and climatology (solid contour line). When the TIO is warmer (or colder) than normal, the SAH strengthens (or weakens) and moves southward (or northward). As TIO SST moves from cold to warm, the center of the SAH shifts southward, its southern boundary moves southward, the eastern and western boundaries respectively shifts eastward and westward, while almost no movement is found in the northern boundary. The definition of the SAH indices follow those in Zhang et al. (2000) and Zhou et al. (2006). The center of the SAH is the grid where the geopotential height is the largest and is expressed by its latitude and longitude. The area of the SAH is the total number of the points where the geopotential height is no less than 16600 m in the region (10°S–50°N, 30°W–180°E). The SAH intensity is the sum of differences between 16600 m and the geopotential height at each point where the geopotential height is no less than 16600 m in that region. The correlation coefficients between the TIO SST and SAH indices (including strengthening index, area index, center latitude and center longitude), are 0.63, 0.53, −0.43 and −0.08, respectively. Among the four correlation coefficients, the first two reach the 99% confidence level and the third reaches the 95% significance level. Thus when the TIO is warmer, not only does the SAH strengthen, but its center and main body also shift southward. However, at the interannual timescale, no direct relationship could be found between TIO SST and zonal displacement of the SAH in boreal summer.
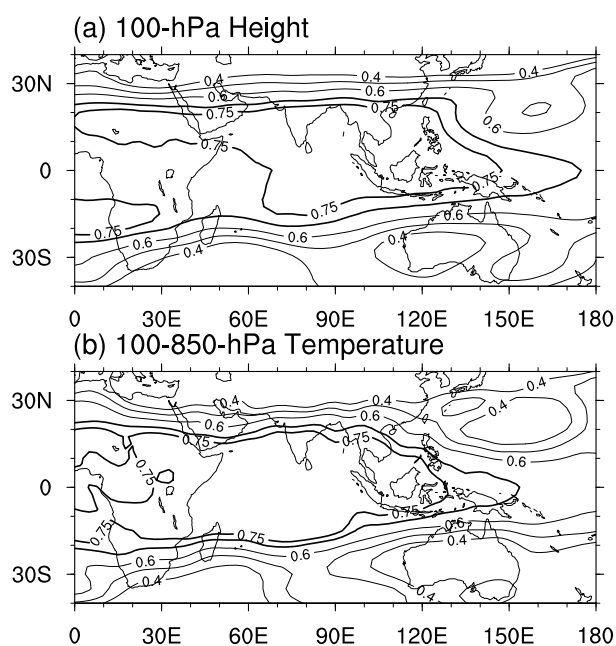
(a) 100-hPa Height

(b) 100-850-hPa Temperature

Fig. 5. Correlation with JJA TIO SST index: (a) 100-hPa geopotential height, (b) tropospheric temperature. The value 0.4, 0.5, 0.6, 0.65, 0.7 and 0.75 are shown in contours, and the value 0.7 and 0.75 are shown in thick contours.

3.2 *Possible mechanism of impact*

Figure 5 shows the correlation distribution of 100-hPa geopotential height (hereafter H100) and tropospheric temperature (100–850-hPa temperature; hereafter TT) with TIO SST. In the H100 field (Fig. 5a), a significant positive anomaly is situated in the tropical and subtropical region over the TIO and surrounding areas. The height anomaly over the domain (15°–30°N, 30°–120°E), south of the SAH's climatological location, is the key area for the strengthening and southward displacement of the SAH in boreal summer. As anomalies of H100 are closely related to the variation in 100–850-hPa temperature, TT field was analyzed. In the TT field (Fig. 5b), to the west of the Indian Ocean, two maximums reside off the equator over tropical Africa; to the east, the maximum lies along the equator over the maritime continents. The TT anomaly over the Indian Ocean and the surrounding regions exhibits a Matsunuo-Gill pattern in response to local heating (thick contours in Fig. 5b), indicating an active area of the TIO on the atmosphere.

Previous studies (Yang et al., 2007; Yang and Liu, 2008) on the impacts of the TIO on the SAH have suggested that condensational heating associated with precipitation anomalies plays an important role in the effects of the TIO on the SAH. However, the correlation results between TIO SST and precipitation do
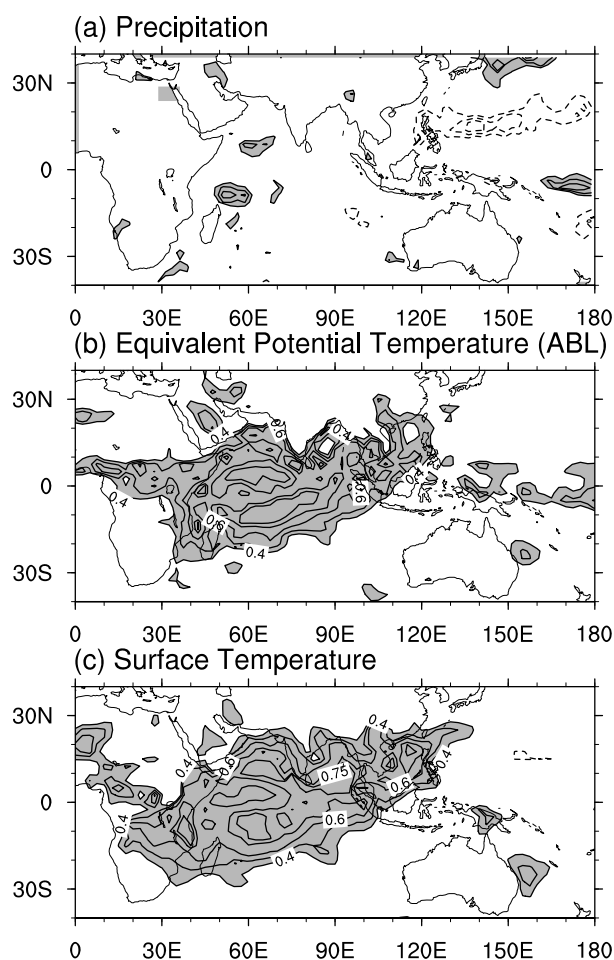
(a) Precipitation

(b) Equivalent Potential Temperature (ABL)

(c) Surface Temperature

Fig. 6. Correlation with JJA TIO SST index: (a) precipitation; (b) EPT in 1000-hPa and (c) surface temperature. Shading indicates values larger than 0.4. The value −0.75, −0.7, −0.6, −0.5, −0.4, 0.4, 0.5, 0.6, 0.65, 0.7 and 0.75 are shown in contours; negative values are shown in dash contours.

not exhibit large scale anomalous rainfall, and significant precipitation anomalies only locate over the southwest Indian Ocean and south Arabian Sea (Fig. 6a). The weak correlation between TIO SST and precipitation in boreal summer has also been pointed out by Xie et al. (2009). For convenience, the area average of H100 in summer over the domain (15°–30°N, 30°–120°E), which is the key area for the strengthening and southward displacement of the SAH, is defined as an index, named SAHSE; also, the area mean of precipitation over the domain (20°S–20°N, 40°–100°E) is defined as an index, named PTIO. The correlation coefficient between SAHSE and PTIO is 0.25, not reaching the 90% significance level. Thus, the correlation analysis indicates that condensational heating associated with local precipitation over the Indian Ocean does not play the key role in the response of the H100.
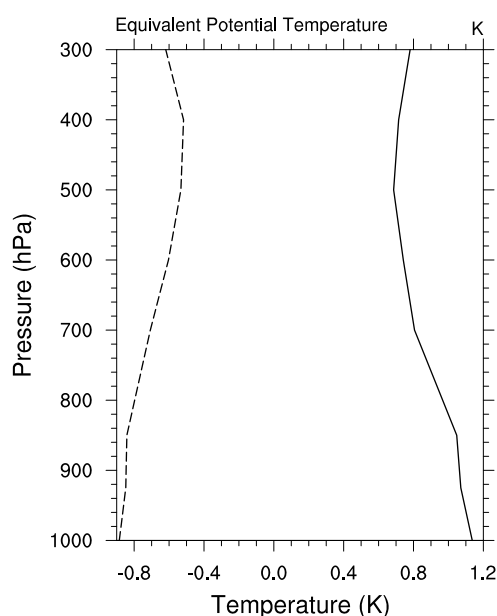
Fig. 7. Anomalous EPT (K) profile over the TIO when the TIO is warm (solid line) and cold (dash line).

In order to better understand the tropospheric warming over the TIO when the TIO is warm, the theory of moist adjustment is introduced. In the tropical wet atmosphere, the temperature profile follows approximately a moist-adiabatic profile which can be determined by moist static energy (MSE) or equivalent potential temperature (EPT) in the atmospheric boundary layer (ABL; Emanuel et al., 1994, 1997; Su and Neelin, 2003). It was pointed out by Xie et al. (2009) that the TIO warms the atmospheric column through modifying the EPT or MSE in the ABL. Figure 7 shows the anomalous EPT profiles when the TIO is warm and cold in boreal summer. As the specific humidity dataset in the NCEP-NCAR reanalysis is limited up to 300 hPa, the EPT profile was calculated between that level and 1000 hPa. Unlike the latent heat profile with a prominent peak at one level, the EPT profile shows an approximate uniform warm (or cold) profile from lower to upper level, further indicating that precipitation-induced latent heat may not play the key role. Correlation of EPT1000 with TIO SST shows a large-scale significant positive anomaly over the TIO (Fig. 6b). The correlation coefficient between the area average of EPT1000 over the domain (20°S–20°N, 40°–100°E) and SAHSE is 0.75, far exceeding that between PTIO and SAHSE. The correlation coefficient reveals that TIO-SST-induced EPT change in the ABL is a more important manner through which TIO SST effects tropospheric warming.

In brief, in boreal summer, the warming of the TIO induces EPT variation in the ABL, modulates the tem-

perature profile of the atmosphere above it, heats the atmospheric column, elevates H100 with a significant positive H100 anomaly to the south of the SAH's climatological location, strengthens the SAH and leads to a southward shift of its center.

Besides the direct influence of the TIO on the SAH, some indirect processes, such as TIO-SST-anomaly-induced anomalous conditions on land and the thermal contrast between land and ocean, may also contribute to variation in the SAH. When the TIO is warm in boreal summer, precipitation increases over the north of the Bay of Bengal (Fig. 6a), in accordance with the simulation results of Yang and Liu (2008). The associated condensational heating contributes to tropospheric warming over the area and forces an anomalous anticyclone in the upper troposphere over the SAH's climatological position. These processes are favorable for the strengthening and southward displacement of the SAH. As the TIO warms, warm anomalies in surface temperature are found in the southwest of the Indian Peninsula, east of the Indian and north of the Indo-China Peninsula (Fig. 6c). It can be inferred that the consequent sensible heat anomaly may also contribute to tropospheric warming. Moreover, TIO warming may reduce the thermal contrast between the Indian Ocean and the continent of Asia, thus height difference over the two regions is reduced and a positive height anomaly occurs over the TIO region. This may also cause a strengthening and southward displacement of the SAH.

4. Model results

AGCM experiments were designed to test the hypothesis that TIO SST affects the strength and latitudinal displacement of the SAH in summer. For convenience, NCEP and CMAP results are referred to as "observation", though the NCEP reanalysis is obviously not observational data.

4.1 *Prediction ability of ECHAM5*

In the observation, summer mean precipitation in climatology locates mainly in the equatorial Indian Ocean, east Arabian Sea, Indian Peninsula and the Bay of Bengal, with a maximum over the equatorial southeast Indian Ocean, west of the Indian Peninsula and northeast of the Bay of Bengal (Fig. 8a). For the summer mean TT field, a ridge exists from northern Madagascar to the Somali Peninsula and two maximums exist over the Iran and Tibet Plateaus (Fig. 8a). In H100, a large-scale high system, the SAH, locates over Iran and Tibet Plateaus, with its center above the Tibet Plateau (Fig. 9a).
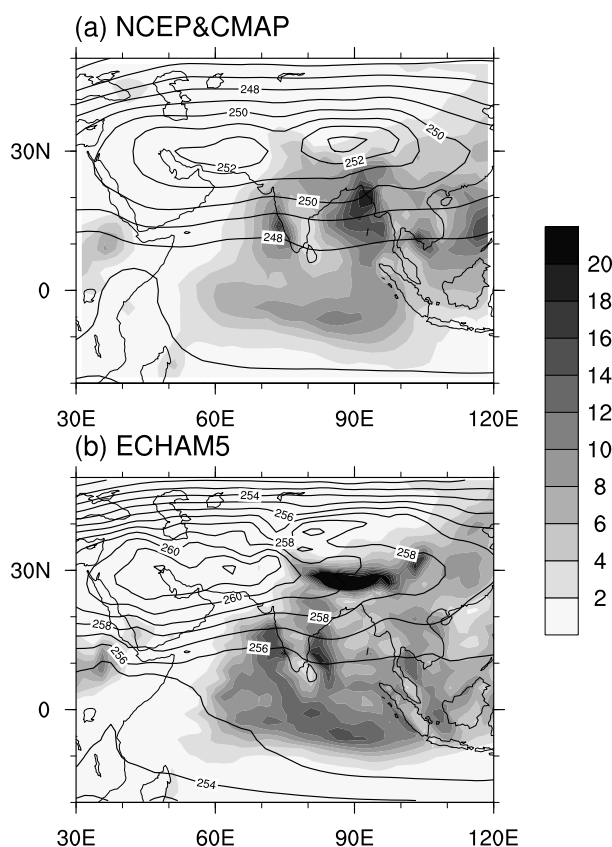
In ECHAM5, the large-scale characteristics of cli-

(a) NCEP&CMAP

(b) ECHAM5

Fig. 8. Climatology of tropospheric temperature (contours) and precipitation (shaded) in JJA, (a) results of NCEP and CMAP; (b) results of ECHAM5. The units of tropospheric temperature and precipitation are K and mm d^{-1}, respectively.

matological precipitation in summer are consistent with those in observation, with large-scale precipitation along the equatorial south Indian Ocean, Arabian Sea and the Bay of Bengal; ECHAM5 also captures well the maximums in the equatorial southeast Indian Ocean and west Indian Peninsula, but fails to capture the maximum in the northeast of the Bay of Bengal (Fig. 8b). In ECHAM5, the TT ridge in the observation is reproduced well and there is also a maximum over 30°N. Although, the maximum shifts westward compared to the observation, and locates over the Iran Plateau (Fig. 8b). The value of simulated H100 is larger than that of the observation, and the SAH is reproduced but shifts westward relative to the observation (Fig. 9b). Therefore ECHAM5 can simulate tropospheric temperature, precipitation and geopotential height near the Indian Ocean well, and the climatology of the SAH is reproduced quite well. It is reasonable to discuss the impact of TIO SST on the strengthening and latitudinal variations of the SAH by using ECHAM5.

Owing to the difference of H100 value between ECHAM5 and the observation, 16860-gpm contour is adopted to characterize the SAH in simulation. Figure 10a illustrates the contour lines for 16860-gpm of 100-hPa geopotential height when JJA TIO SST is warm, cold and climatological. As the TIO warms (or cools), the SAH strengthens (or weakens) and shifts slightly southward (or northward), consistent with observed results.

4.2   *The TIO sensitivity experiment*

In order to investigate the effect of TIO SST alone and exclude the influences of SST over other oceans, TIOSE was analyzed. Figure 10b illustrates contour lines for 16860 gpm of 100-hPa geopotential height when the SSTA imposed on the TIO is 0–1 K and 1–2 K mean. Compared to the results of 0–1 K mean, the SAH strengthens and expands southward when the TIO SSTA is 1–2 K mean, with more significant movement in the southern boundary than that in the northern boundary. The SAH indices in this experiment were defined according to the definition in Zhang et al. (2000) and Zhou et al. (2006), except that the characteristic contour is 16 860 gpm. The scatter plots of SAH intensity (Fig. 11a), area (Fig. 11b) and center latitude (Fig. 11c) in TIOSE show good linear relation with SSTAs imposed on the TIO (the linear regression of all three reach the 99.9% significance level), while the linear relationship between center longitude and SSTA is poor (Fig. 11d). The results are well in accordance with the relationship between the TIO and SAH variation in the observation.

Figure 12 shows the differences in H100, TT, precipitation and EPT1000 between 1–2 K SSTA mean and 0–1 K SSTA mean. The H100 field (Fig. 12a) shows a significant positive height anomaly extending northward to 40°N. The height anomaly decreases from tropics to the mid latitude, leading to more significant movement in the SAH's southern boundary than in its northern boundary, as well as the southward displacement of its center. The response of TT shows two maximums off the equator, one to the west of the Indian Ocean and the other along the equator (Fig. 13b), which features a Matsuno-Gill type response. EPT1000 shows a large-scale significant positive anomaly over the TIO, also in good accordance with the observation (Fig. 12d). The results of H100, TT and EPT1000 support the notion that the TIO warms the troposphere through modulating EPT or MSE in the ABL, strengthens the SAH and makes it expand southward.

Compared to observations, the simulated precipitation is different, with a significant positive precipitation anomaly over the east Indian Ocean, and a
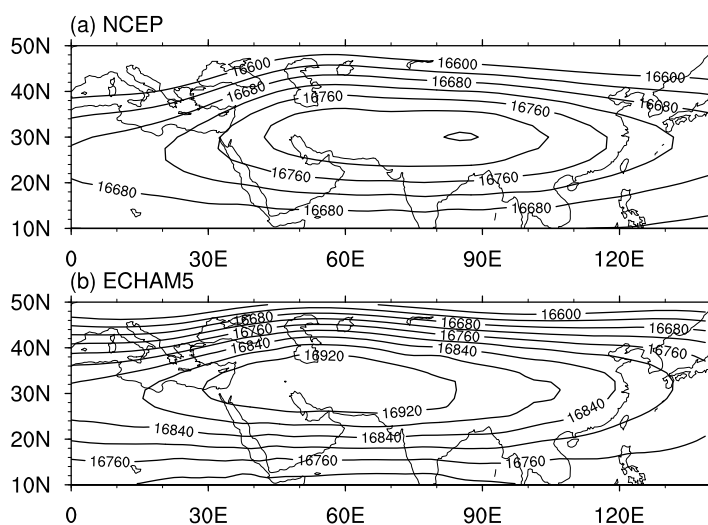
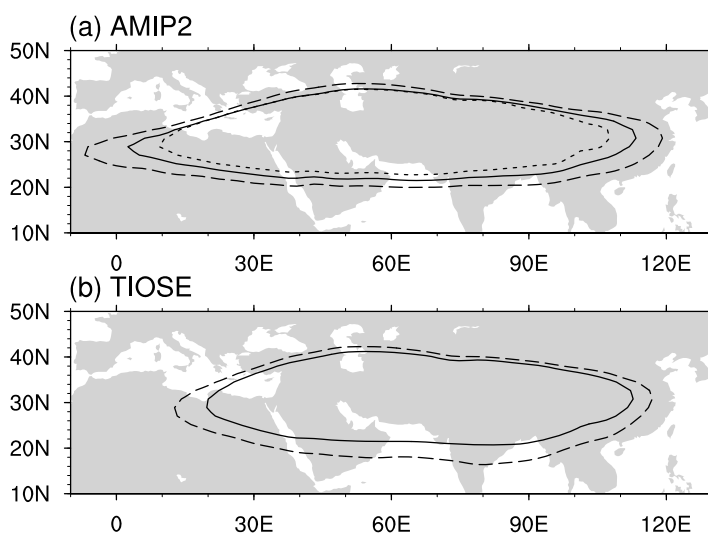**Fig. 9.** Climatology of 100-hPa geopotential height (m) in JJA: (a) NCEP, (b) ECHAM5.

Fig. 10. (a) As Fig. 5, except for 16 860 gpm contour lines in AMIP2 run of ECHAM5. (b) Contour lines for 16 860 gpm of 100-hPa geopotential height when summer TIO SSTA is 0–1 K (solid contour lines) and 1–2 K (dashed contour lines).

negative anomaly over central North Africa from 10°–20°N, Tanzania, the Bay of Bengal and the maritime continents (Fig. 12c). Although the precipitation response over the Bay of Bengal in TIOSE is opposite to that in observations, the SAH strengthens and shifts southward in both TIOSE and the observations. So compared to the effects of precipitation over the Bay of Bengal, another process may be more important to the response of the SAH.

Su and Neelin (2003) pointed out that assuming remote SST is fixed, as local SST increases, moisture in atmospheric boundary adjusts quickly, the temper-ature profile of the atmosphere changes, convective available potential energy increases, and convective precipitation occurs, making the actual temperature profile close to a moist-adiabatic profile, meaning the atmosphere tends to be stable. Convection acts as a key factor in modulating actual temperature close to a moist-adiabatic profile. Thus there is a good relationship between precipitation and SSTAs under these condition. However, in the observation, when the TIO is warm in summer, a SSTA also exists over other oceans (Fig. 1). Provided the TIO SSTA is fixed, SSTAs outside the Indian Ocean may affect the
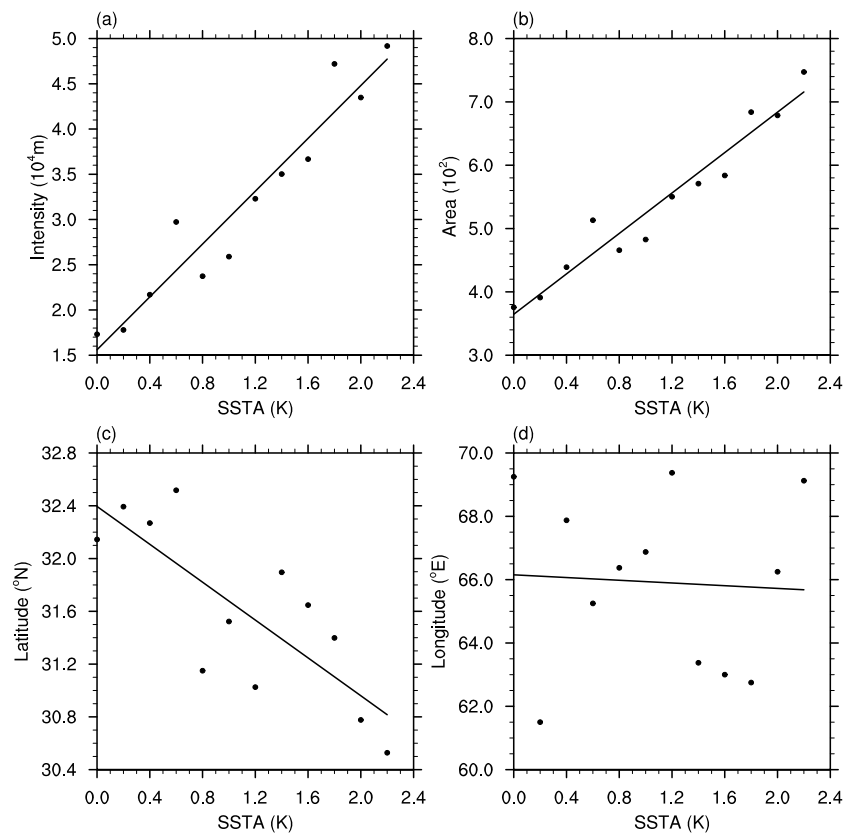
Fig. 11. Scatter plots of SAH (a) intensity ($\times 10^4$ m), (b) area ($\times 10^2$), (c) center latitude (°N) and (d) center longitude (°E) in JJA with respect to SSTA in TIOSE. Linear lines in the four plots are the linear fit lines.
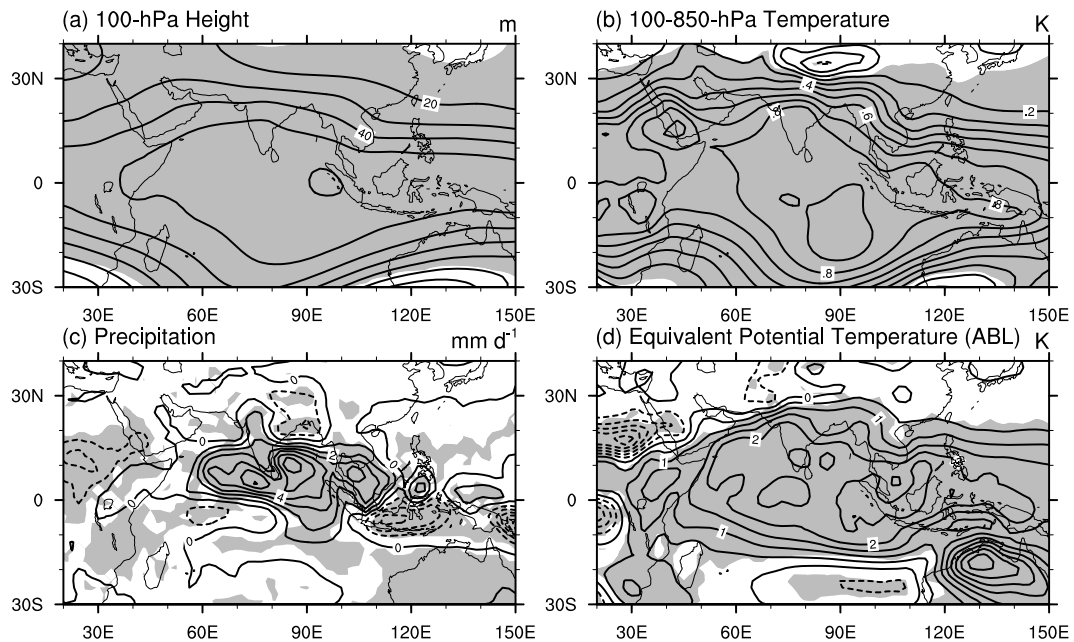

Fig. 12. Differences between 1–2 K mean and 0–1 K mean in TIOSE: (a) 100-hPa geopotential height (m); (b) tropospheric temperature (K); (c) precipitation (mm d^{-1}) and (d) EPT at 1000-hPa (K). Shading indicates the values reaching the 95% significance level. For the sake of clarity, spatial 9-point smoothing is performed.

atmosphere over the Indian Ocean, tending to make it warmer or colder. As the TIO SSTA is fixed, an anomalous EPT in the ABL over the TIO varies very little. From the changes in the vertical temperature profile, the atmosphere over the TIO tends to be more stable or unstable than normal and decreased or increased precipitation occurs to modulate the atmosphere to a neutral state. If the heating of the Indian Ocean is taken into consideration, a warm (or cold) TIO makes the actual temperature profile get close to a moisture-adiabatic profile through increased (or decreased) convective heating. Due to the combined effects of SSTAs over the TIO and outside the TIO, precipitation over the TIO is not significant. Thus the impacts of other oceans on TT over the TIO may account for the insignificant precipitation when the TIO is warm and it is not difficult to understand that precipitation does not necessarily correlate well to local SST. Despite that, the mechansim that the TIO warms the troposphere through modulating EPT or MSE in the ABL and affects the SAH can be applied to explain the results in both TIOSE and the observation. The heat budget of the troposphere over the TIO is still not understood and needs further investigation.

5. Discussion and summary

The effects of TIO SSTA on variations of the SAH and the possible underlying mechanism have been investigated. In the summer when the ENSO decays, the SST and circulation anomalies indicate that TIO SST directly or indirectly plays an active role in circulation changes over the TIO, with an active role by the eastern Pacific not being obvious. This phenomenon is not obvious in spring, nor the preceding winter. Thus the impact of TIO SST in summer was the focus of this study.

Compared to cold cases, when the TIO warms in summer, the main body of the SAH becomes larger, the SAH intensifies and its center shifts southward. A significant correlation can be found between TIO SST and the indices (intensity, area and center latitude) of the SAH, while the relationship between TIO SST and the SAH center longitude is poor. When the TIO warms, the whole troposphere over the TIO is heated with a Matsunuo-Gill response in the troposphere. No significant large-scale precipitation anomaly can be found over the TIO, indicating that precipitation does not act as a key factor in forcing the Matsunuo-Gill response. Emanual et al. (1994, 1997) and Su and Neelin (2003) pointed out that, the temperature in the tropical atmosphere follows approximately a moist-adiabatic profile which is determined by EPT or MSE in the ABL. TIO SST modulates tropospheric

temperature through changing the EPT or MSE in the ABL, forcing the Matsunuo-Gill response. As the TIO warms, because of the spread of tropospheric warming and the Rossby wave response over the northern Indian Ocean, a positive height anomaly occurs in the south of the SAH's climatological location in summer, making the SAH intensify and its center move southward.

AGCM ECHAM5, with a resolution of T63L19, was used to test the effects of TIO SST on variations in the SAH. The model experiment indicated that, as the summer TIO SSTA increases, the SAH strengthens and its center shifts southward significantly. When the TIO warms, a significant tropospheric warm anomaly locates over tropics and subtropics, featuring a Matsuno-Gill type response over the TIO, consistent with the observation. However, the precipitation response to the TIO SSTA is different to that in the observation. By using the theory proposed by Su and Neelin (2003) and analyzing the results obtained in the present study, it can be inferred that when the TIO is warm, SST in other oceans may make a positive or negative contribution to precipitation over the TIO. Thus precipitation over the TIO is not all determined by local SST and the influences of SSTs in other oceans may account for the insignificant precipitation over the TIO in the observation. Although simulated precipitation was different from observed precipitation, the simulation results can still be explained by the mechanism that the TIO warms the troposphere through the modulation of the temperature profile and has impact on the SAH.

The simulations have shown that TIO warming contributes to the strengthening and southward displacement of the SAH in summer. However, the correlation coefficient between the SAH center latitude and simultaneous NINO3.4 index is −0.45, a little higher than that between TIO SST and the SAH center latitude. Therefore, besides the influence of the TIO, a simultaneous influence of eastern Pacific SST may also contribute to the latitudinal movement of the SAH in summer. How the former affects the latter also need further study.

REFERENCES

Alexander, M. A., I. Bladé, M. Newman, J. R. Lanzante, N. C. Lau, and J. D. Scott, 2002: The atmospheric bridge: The influence of ENSO teleconnections on air–sea interaction over the global oceans. *J. Climate*, **15**, 2205–2231.

Annamalai, H., P. Liu, and S.-P. Xie, 2005: Southwest Indian Ocean SST variability: Its local effect and remote influence on Asian monsoons. *J. Climate*, **18**, 4150–4167.

Dethof, A., A. O'Neill, J. M. Slingo, and H. G. J. Smit, 1999: A mechanism for moistening the lower stratosphere involving the Asian summer monsoon. *Quart. J. Roy. Meteor. Soc.*, **125**, 1079–1106.

Du, Y., and S. P. Xie, 2008: Role of atmospheric adjustments in the tropical Indian Ocean warming during the 20th century in climate models. *Geophys. Res. Lett.*, **35**, L08712, doi: 10.1029/2008GL033631.

Du, Y., S. P. Xie, G. Huang, and K. Hu, 2009: Role of air–sea interaction in the long persistence of El Niño–induced North Indian Ocean warming. *J. Climate*, **22**, 2023–2038.

Emanuel, K. A., J. D. Neelin, and C. S. Bretherton, 1994: On large-scale circulations in convecting atmospheres. *Quart. J. Roy. Meteor. Soc.*, **120**, 1111–1143.

Emanuel, K. A., J. D. Neelin, and C. S. Bretherton, 1997: Reply to comments by Bjorn Stevens, David A. Randall, Xin Lin and Michael T. Montgomery on "On large-scale circulations in convecting atmospheres". *Quart. J. Roy. Meteor. Soc.*, **123**, 1779–1782.

Flohn, H., 1960: Recent investigations on the mechanism of the "Summer Monsoon" of Southern and Eastern Asia. *Proc. Symp. Monsoon of the World*, New Delhi, Hind Union Press, 75–88.

Huang, B., and J. L. Kinter, 2002: Interannual variability in the tropical Indian Ocean. *J. Geophys. Res.*, **107**, 3199, doi: 10.1029/2001JC001278.

Kalnay, E., and Coauthors, 1996: The NCEP/NCAR 40-Year Reanalysis Project. *Bull. Amer. Meteor. Soc.*, **77**, 437–471.

Klein, S. A., B. J. Soden, and N. C. Lau, 1999: Remote sea surface temperature variations during ENSO: Evidence for a tropical atmospheric bridge. *J. Climate*, **12**, 917–932.

Lau, N. C., and M. J. Nath, 2000: Impact of ENSO on the variability of the Asian–Australian monsoons as simulated in GCM experiments. *J. Climate*, **13**, 4287–4309.

Lau, N. C., and M. J. Nath, 2003: Atmosphere-Ocean variations in the Indo-Pacific sector during ENSO episodes. *J. Climate*, **16**, 3–20.

Li, Q., and Coauthors, 2005: Convective outflow of South Asian pollution: A global CTM simulation compared with EOS MLS observations. *Geophys. Res. Lett.*, **32**, L14826, doi: 10.1029/2005GL022762.

Li, S., J. Lu, G. Huang, and K. Hu, 2008: Tropical Indian Ocean basin warming and East Asian summer monsoon: A multiple AGCM study. *J. Climate*, **21**, 6080–6088.

Mason, R. B., and C. E. Anderson, 1963: The development and decay of the 100-MB. Summertime anticyclone over Southern Asia. *Mon. Wea. Rev.*, **91**, 3–12.

Masumoto, Y., and G. Meyers, 1998: Forced Rossby waves in the southern tropical Indian Ocean. *J. Geophys. Res.*, **103**, 27589–27602.

Park, M., W. J. Randel, D. E. Kinnison, R. R. Garcia, and W. Choi, 2004: Seasonal variation of methane, water vapor, and nitrogen oxides near the tropopause: Satellite observations and model simulations. *J. Geophys. Res*, **109**, D03302, doi: 10.1029/2003JD003706.

Randel, W. J., and M. Park, 2006: Deep convective influence on the Asian summer monsoon anticyclone and associated tracer variability observed with Atmospheric Infrared Sounder (AIRS). *J. Geophys. Res.*, **111**, D12314, doi: 10.1029/2005JD006490.

Rayner, N. A., P. Brohan, D. E. Parker, C. K. Folland, J. J. Kennedy, M. Vanicek, T. J. Ansell, and S. F. B. Tett, 2006: Improved analyses of changes and uncertainties in sea surface temperature measured in situ since the mid-nineteenth century: The HadSST2 dataset. *J. Climate*, **19**, 446–469.

Roeckner, E., and Coauthors, 2003: The atmospheric general circulation model ECHAM5: Part 1: Model description. Max-Planck-Institut für Meteorologie Rep. 349, 140pp.

Su, H., and J. D. Neelin, 2003: The scatter in tropical average precipitation anomalies. *J. Climate*, **16**, 3966–3977.

Tao, S., and F. Zhu, 1964: The variation of 100mb circulation over South Asia in summer and its association with march and withdraw of West Pacific Subtropical High. *Acta Meteorological Sinica*, **34**, 385–395. (in Chinese)

Wang, B., R. Wu, and X. Fu, 2000: Pacific–East Asian teleconnection: How does ENSO affect East Asian climate? *J. Climate*, **13**, 1517–1536.

Wang, B., R. Wu, and T. Li, 2003: Atmosphere-warm ocean interaction and its impacts on Asian-Australian monsoon variation. *J. Climate*, **16**, 1195–1211.

Wu, B., T. Zhou, and T. Li, 2009: Seasonally evolving dominant interannual variability modes of East Asian climate. *J. Climate*, **22**, 2992–3005.

Xie, P., and P. A. Arkin, 1997: Global precipitation: A 17-year monthly analysis based on gauge observations, satellite estimates, and numerical model outputs. *Bull. Amer. Meteor. Soc.*, **78**, 2539–2558.

Xie, S.-P., H. Annamalai, F. A. Schott, and J. P. McCreary, 2002: Structure and mechanisms of South Indian Ocean climate variability. *J. Climate*, **15**, 864–878.

Xie, S.-P., K. Hu, J. Hafner, H. Tokinaga, Y. Du, G.

Huang, and T. Sampe, 2009: Indian Ocean capacitor effect on Indo–Western Pacific climate during the Summer following El Niño. *J. Climate*, **22**, 730–747.

Xie, S.-P., Y. Du, G. Huang, X.-T. Zheng, H. Tokinaga, K. Hu, and Q. Liu, 2010: Decadal shift in El Niño influences on Indo-western Pacific and East Asian climate in the 1970s. *J. Climate*, **23**, 3352–3368.

Yang, J., Q. Liu, S. P. Xie, Z. Liu, and L. Wu, 2007: Impact of the Indian Ocean SST basin mode on the Asian summer monsoon. *Geophys. Res. Lett.*, **34**, L02708, doi: 10.1029/2006GL028571.

Yang, J., and Q. Liu, 2008: The "charge/discharge" role of the basin-wide mode of the Indian Ocean SST anomaly-influence on the South Asian High in summer. *Acta Oceanologica Sinica*, **30**, 12–19. (in Chinese)

Yu, W., B. Xiang, L. Liu, and N. Liu, 2005: Understanding the origins of interannual thermocline variations in the tropical Indian Ocean. *Geophys. Res. Lett.*, **32**, L24706, doi: 10.1029/2005GL024327.

Zhang, P., S. Yang, and V. E. Kousky, 2005: South Asian High and Asian-Pacific-American Climate Teleconnection. *Adv. Atmos. Sci.*, **22**, 915–923.

Zhang, Q., Y. Qian, and X. Zhang, 2000: Interannual and Interdecadal variations of the South Asia High. *Chinese J. Atmos. Sci.*, **24**, 67–78. (in Chinese)

Zhang, Q., and G. Wu, 2001: The large area flood and drought over Yangtze river valley and its relation to the South Asia High. *Acta Meteorologica Sinica*, **59**, 569–577. (in Chinese)

Zhang, Q., G. Wu, and Y. Qian, 2002: The bimodality of the 100 hPa South Asia high and its relationship to the climate anomaly over East Asia in summer. *J. Meteor. Soc. Japan*, **80**, 733–744.

Zhao, P., X. Zhang, Y. Li, and J. Chen, 2009: Remotely modulated tropical-North Pacific ocean–atmosphere interactions by the South Asian high. *Atmos. Res.*, **94**, 45–60.

Zhou, N., Y. Yu, and Y. Qian, 2006: Simulation of the 100-hPa South Asian High and precipitation over East Asia with IPCC coupled GCMS. *Adv. Atmos. Sci.*, **23**, 375–390.